



**HAL**  
open science

# Multiple Harmonic Current Injection System for Audible Noise Analysis of AC Filter Capacitors in Converter Stations

Jingang Han, Shouzhi Zheng, Gang Yao, Hao Chen, Yide Wang, Tianhao Tang

► **To cite this version:**

Jingang Han, Shouzhi Zheng, Gang Yao, Hao Chen, Yide Wang, et al.. Multiple Harmonic Current Injection System for Audible Noise Analysis of AC Filter Capacitors in Converter Stations. IEEE Access, 2020, 8, pp.94024-94032. 10.1109/ACCESS.2020.2993458. hal-02569098

**HAL Id: hal-02569098**

**<https://hal.science/hal-02569098>**

Submitted on 17 Jul 2020

**HAL** is a multi-disciplinary open access archive for the deposit and dissemination of scientific research documents, whether they are published or not. The documents may come from teaching and research institutions in France or abroad, or from public or private research centers.

L'archive ouverte pluridisciplinaire **HAL**, est destinée au dépôt et à la diffusion de documents scientifiques de niveau recherche, publiés ou non, émanant des établissements d'enseignement et de recherche français ou étrangers, des laboratoires publics ou privés.



Distributed under a Creative Commons Attribution 4.0 International License

Received March 9, 2020, accepted April 28, 2020, date of publication May 8, 2020, date of current version June 2, 2020.

Digital Object Identifier 10.1109/ACCESS.2020.2993458

# Multiple Harmonic Current Injection System for Audible Noise Analysis of AC Filter Capacitors in Converter Stations

JINGANG HAN<sup>1</sup>, (Member, IEEE), SHOUZHI ZHENG<sup>1</sup>, GANG YAO<sup>1</sup>, (Member, IEEE),  
HAO CHEN<sup>1</sup>, (Member, IEEE), YIDE WANG<sup>1,2</sup>, (Senior Member, IEEE),  
AND TIANHAO TANG<sup>1</sup>, (Senior Member, IEEE)

<sup>1</sup>Institute of Electric Drives and Control Systems, Shanghai Maritime University, Shanghai 201306, China

<sup>2</sup>IETR-UMR CNRS 6164, l'Universite de Nantes, 44300 Nantes, France

Corresponding author: Jingang Han (jghan@shmtu.edu.cn)

This work was supported in part by the National Natural Science Foundation of China under Grant 61673260 and Grant 61503242.

**ABSTRACT** The audible noise of AC filter capacitors is one of the major noise sources in High Voltage Direct Current (HVDC) converter stations. In order to avoid the sharp noise of AC filter capacitors, it is necessary to design a Multiple Harmonic Current Injection System (MHCIS) for power capacitors to analyze their audible noise characteristics. Simulating effectively the noise of AC filter capacitors under their actual working conditions in converter stations is the primary target of this proposed MHCIS. To ensure the accuracy of the harmonic currents injected into the power capacitors, each harmonic current is detected and controlled separately. On the basis of the instantaneous reactive power theory, a selective harmonic current detection algorithm is proposed in this paper for the single-phase MHCIS. The amplitude of the selected harmonic current can be tracked timely and exactly in  $d$ - $q$  synchronous rotational coordinate system, such that a Proportional Integral (PI) controller can be directly operated to eliminate the steady-state errors. The experimental parameters are usually invariable in this system, the phase deviation of the selected harmonic current is also fixed. Thus the phase angle offset of the corresponding harmonic current can be detected and calculated to compensate the system inherent delay. Owing to the accurate detection and control of multiple harmonic currents, the actual working conditions of AC filter capacitors can be accurately simulated, and the reliable noise analysis results of power capacitors can be obtained. Finally, the proposed selective harmonic current detection and control algorithm is verified by the theoretical analysis, simulation and experimental results.

**INDEX TERMS** AC filter capacitor, current control, harmonic current, synchronous rotating frame.

## I. INTRODUCTION

High Voltage Direct Current (HVDC) power networks are widely applied in modern power grids, because of their ability of flexible control of DC and significant potential for long-distance, high-capacity power transmission of regional grids [1]. However, in HVDC converter stations, AC filter capacitors generate audible harsh noise due to the flowing multiple harmonic currents. The audible noise generation mechanism and the relation between the harmonic currents and audible noise are studied in [2]–[4]. Briefly, when the multiple harmonic currents flow through the power capacitor

unit, the internal electric forces will cause the external mechanical vibration, resulting in the harsh audible noise of power capacitors.

In order to achieve the precise analysis results of noise and vibration characteristics of power capacitors, it is necessary to simulate effectively the working conditions of AC filter capacitors. As the system impedance is different for different harmonic current, different frequency signals will have different characteristics. Besides, the AC filter capacitors' noise characteristics are proved to be related to the current frequency, magnitude and relative phase angle [5]. Therefore, in order to achieve the accurate result of noise analysis for AC filter capacitors, it is the most critical task to design a Multiple Harmonic Current Injection System (MHCIS), in which the

The associate editor coordinating the review of this manuscript and approving it for publication was Enamul Haque.

relative phase angle and magnitude of each harmonic current can be detected and controlled.

How to detect the harmonic current quickly and accurately in real-time is a pivotal part for MHCIS. A series of current detection methods have been presented. Some methods in frequency domain based on Fourier analysis are described in [6]–[8]. Meanwhile, a lot of harmonic current detection algorithms based on the instantaneous reactive power theory have been proposed in time domain [9], such as  $p$ - $q$  [10], [11] and  $d$ - $q$  [12] methods. Jing *et al.* [13] have introduced a random harmonic current detection strategy to identify the positive and negative sequence component of random harmonic current. In two-phase stationary frame, a harmonic and reactive current detection strategy without using any coordinate transformation is proposed in [14].

In this paper, the proposed selective harmonic current detection algorithm is also based on the theory of instantaneous reactive power.

The current regulation approaches in  $\alpha$ - $\beta$  stationary frame based on the Proportional Resonant (PR) controller are discussed in [15], [16]. PR controllers can offer infinite gain for AC components at the specified frequency, thus can eliminate the steady-state errors when tracking an AC reference. Meanwhile, due to the fact that the magnitude obtained in synchronous rotating coordinate system is DC components, the Proportional Integral (PI) controller can be directly used in  $d$ - $q$  synchronous rotating frame to offer an infinite gain for DC components [17], [18]. Besides that, P. Mattavelli *et al.* at [19] have proposed a repetitive-based controller to compensate the selected harmonic current. As the phase angle of harmonic will affect the results of the harmonic compensation, a selective harmonic compensation method based on the dynamic phasor theory is proposed in active power filtering [20]. And an active compensation method through the jittering of selective harmonic elimination phase angle is applied to high-power PWM converters' system [21].

In this paper, a selective harmonic current control algorithm based on the PI controller in multiple synchronous rotating frames is proposed. The phase deviation of each considered harmonic current is detected and calculated to compensate the impact of the system inherent delay. After the control of magnitude and compensation of phase angle offset of the selected harmonic current in multiple synchronous rotating frames, the output harmonic current can be realized by inverse transformation.

This paper proposes a Multiple Harmonic Current Injection System (MHCIS) for noise analysis of AC filter capacitors in converter stations. Firstly, the simplified configuration of the proposed system is introduced, and the system modeling is built. Then the proposed harmonic current detection algorithm is described based on the theory of instantaneous reactive power. The amplitude and phase angle of each selected harmonic current can be calculated. After that, the PI current controller in multiple synchronous coordinate systems is designed for each selected harmonic

TABLE 1. Harmonic currents distribution.

Harmonic order	frequency/Hz	I/A
1	50	74.99
5	250	8.625
7	350	28.55
9	450	5.55
11	550	9.20
13	650	91.3

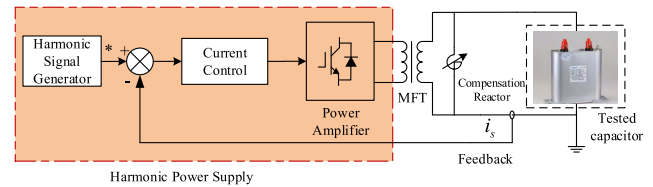


FIGURE 1. Structure block of MHCIS.

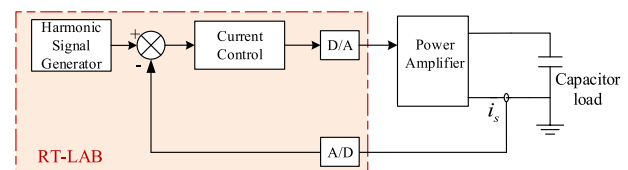


FIGURE 2. Simplified test bench of MHCIS.

current. Finally, the experimental results obtained by RT-LAB platform are presented to verify the feasibility of the proposed selective harmonic current detection and control strategy.

## II. SYSTEM CONFIGURATION AND MODELING

The block diagram of MHCIS is shown in Fig.1 [22], [23], which consists of harmonic power supply, tested capacitors, current transformer and control module, power amplifier, compensation reactor and medium frequency transformer (MFT).

The harmonic power supply can generate the specified fundamental current and associated harmonic currents. The parameters of each harmonic current, such as the reference amplitude and the phase angle, can be designed in the harmonic signal generator module. Table 1 shows the measured values of harmonic currents for a power capacitor in a converter station, which can be used as the reference values of the system. The measured capacitor is of  $38.5\mu\text{F}$  capacitance,  $6.2\text{kV}$  rated voltage.

### A. MODEL OF MULTIPLE HARMONIC CURRENT INJECTION SYSTEM

A simplified test bench of MHCIS, shown in Fig.2, is built in this work due to the limitation of laboratory. The low voltage AC film capacitors replace the AC filter capacitors, which are used as the tested capacitors, the compensation reactor and the MFT are removed.

The power amplifier used in this system has its own voltage and current closed-loop control. The power amplifier can be modeled, approximately, as a first-order inertia system, and

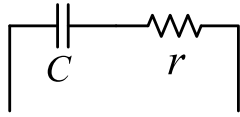


FIGURE 3. Model of the tested capacitor.

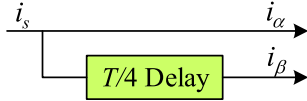


FIGURE 4. T/4 delay block.

the transfer function can be written as:

$$G_{AMP} = \frac{k_{PWM}}{1 + s\tau} \quad (1)$$

where  $k_{PWM}$  is the proportional coefficient of the power amplifier, and  $\tau$  is the inertia time constant, which is usually related to the sampling delay.

The tested capacitors can be considered as a series circuit of resistor  $r$  and capacitor  $C$ , as shown in Fig.3.

The transfer function between the capacitor current  $I_C(s)$  and voltage  $U_C(s)$  is expressed as

$$\frac{I_C(s)}{U_C(s)} = \frac{sC}{sCr + 1} \quad (2)$$

### B. SELECTIVE HARMONIC CURRENT DETECTION STRATEGY

The single-phase selective harmonic current detection strategy designed in this paper for MHCIS is based on the multiple synchronous rotating frame transformation principle and instantaneous reactive power theory.

The transformation matrix cannot be directly used in a single-phase system, due to the lack of the orthogonal current signals. Thus a lot of studies about how to create the quadrature signal from the original single-phase system have been proposed [24], among which the most popular method is the  $T/4$  delay block (one-quarter of a period) for orthogonal signal generator (OSG), owing to its simple digital implementation, as shown in Fig.4.

$$\begin{cases} i_\alpha = i \sin(\theta) \\ i_\beta = i \sin(\theta + T/4n) = i \cos(\theta) \\ \theta = n\omega t + \varphi \end{cases} \quad (3)$$

where  $i_\alpha$  is the original signal and  $i_\beta$  is generated by the  $T/4$  delay block,  $T$  is the fundamental period for  $\omega = 100\pi$ ,  $n$  is the harmonic order, and can take the values of 1, 3, 5, 7, ...

The traditional synchronous rotating frame is extended to the specified frequency synchronous rotating frame based on the instantaneous reactive power theory. The  $n^{\text{th}}$  synchronous rotating frame is taken for example. The  $\alpha$ - $\beta$  frame is always stationary, while the  $d$ - $q$  rotating coordinate system is rotated with angular frequency  $n\omega$ , which is the angular velocity for the  $n^{\text{th}}$  harmonic current. The DC components

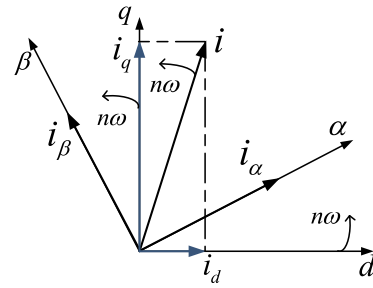


FIGURE 5. Relationship between the stationary and rotating reference frames.

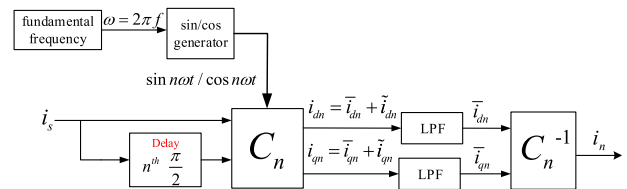


FIGURE 6.  $n^{\text{th}}$  frequency current detection algorithm.

( $i_{dn}$ , and  $i_{qn}$ ) can be obtained via the specified frequency synchronous rotating frame transformation. The  $n^{\text{th}}$  synchronous rotating frame transformation matrix is defined as:

$$C_n = \begin{bmatrix} \cos(n\omega t) & \sin(n\omega t) \\ -\sin(n\omega t) & \cos(n\omega t) \end{bmatrix} \quad (4)$$

The relationship between the stationary and the  $n^{\text{th}}$  synchronous rotating coordinate system is shown in Fig. 5, where  $n\omega$  is the angular frequency for the  $n^{\text{th}}$  harmonic current.

The selected harmonic current is converted into the DC value via the synchronous rotating coordinate system at the corresponding frequency, while the currents at other harmonic orders are always AC quantities via the same synchronous rotating frame transformation matrix. Therefore two Low-Pass Filters (LPFs) are added in the synchronous rotating frame to filter the AC quantities. Hence the DC components for the  $n^{\text{th}}$  harmonic current can be acquired, as shown in Fig. 6. Then the selected harmonic current without any other harmonic order components can be obtained again through the corresponding inverse transformation matrix, defined as:

$$C_n^{-1} = \begin{bmatrix} \cos(n\omega t) & -\sin(n\omega t) \\ \sin(n\omega t) & \cos(n\omega t) \end{bmatrix} \quad (5)$$

Fig.7 shows the flow chart of the selective harmonic current detection algorithm for MHCIS proposed in this paper, and the detection algorithm for the fundamental current is taken for example. The DC components obtained after the two LPFs are  $\bar{i}_{d1}$  and  $\bar{i}_{q1}$ , the amplitude of the fundamental current  $i_1$  can be calculated by  $\sqrt{\bar{i}_{d1}^2 + \bar{i}_{q1}^2}$ . The corresponding phase angle  $\varphi_1$  can be calculated as:

$$\varphi_1 = \arctan(\bar{i}_{q1}/\bar{i}_{d1}) \quad (6)$$

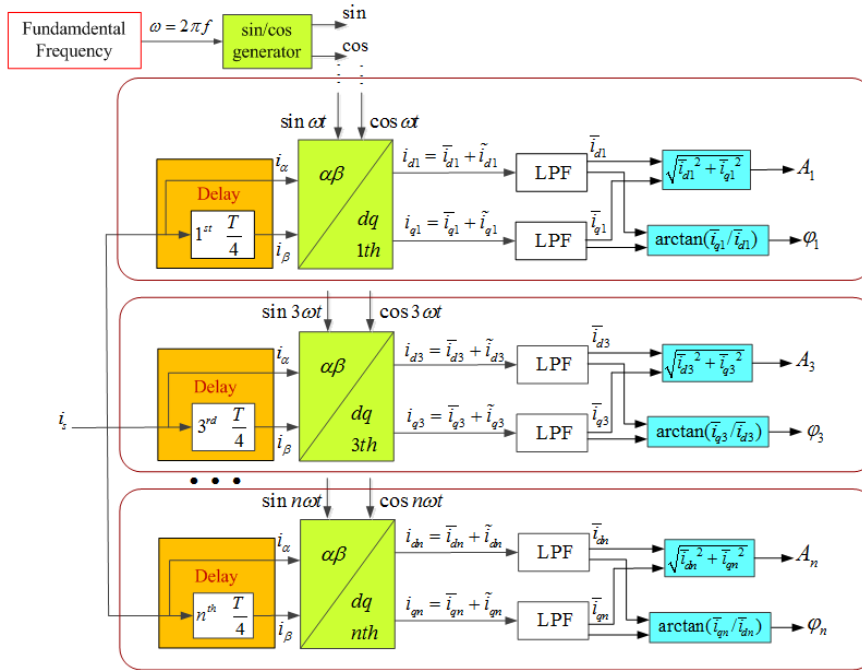


FIGURE 7. Harmonic current detection method.

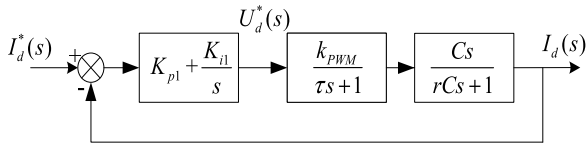


FIGURE 8. Fundamental current closed-loop control diagram.

### C. HARMONIC CURRENT CONTROL STRATEGY

In multiple synchronous rotating coordinate system, the harmonic currents are transformed into DC quantities and PI controllers can be used directly to eliminate the steady-state errors.

The  $n^{\text{th}}$  PI controller for the  $n^{\text{th}}$  harmonic current in the multiple synchronous rotating frame has the following standard transfer function:

$$H_n(s) = K_{pn} + \frac{K_{in}}{s} \quad (7)$$

where  $K_{pn}$  and  $K_{in}$  are the proportional and integral coefficients respectively for the  $n^{\text{th}}$  harmonic current,  $n$  can take the values of 1, 3, 5, . . . ,  $h$ , and  $h$  is the harmonic order.

The new control variables  $U_d^*$ ,  $U_q^*$  which are the reference voltages of PI controllers for fundamental current, are defined. Take only the  $d$ -axis frame into account, the transfer function of the system can be expressed as:

$$U_d^* \frac{k_{PWM}}{s\tau + 1} = I_d(s) \frac{sCr + 1}{sC} \quad (8)$$

where  $I_d(s)$  is the amplitude of the fundamental current. Fig.8 shows the current control model of the system under

the fundamental frequency synchronous rotating coordinate system.

Thus the open-loop transfer function of the fundamental current can be expressed as:

$$G(s) = \frac{K_{p1}(s + K_{i1}/K_{p1})}{s} \cdot \frac{k_{PWM}Cs}{rC\tau s^2 + (rC + \tau)s + 1} \quad (9)$$

Considering the dynamic response and robustness of the system, we can let the value of bandwidth  $\omega_p$  equals to 5-10 times  $\omega_0$ , where  $\omega_0$  is the fundamental angular frequency. Then selecting an appropriate phase margin for this system, the values of the proportional coefficient  $K_{p1}$  and integral coefficient  $K_{i1}$  for the fundamental current can be calculated with the help of Bode diagram [25]–[27].

In order to remedy the impact of the system inherent delay, a phase angle compensation segment is included in the control loop. Since the parameters of this system are usually invariable in the experiment, the phase angle offset of the selected harmonic current is also constant. The operation flow of MHCIS is shown in Fig. 9. In the pretreatment segment, the phase deviation  $\Delta\varphi_n$  can be detected and calculated to compensate the phase angle for the corresponding harmonic current. Hence  $C_n^{-1}$  becomes:

$$C_n^{-1} = \begin{bmatrix} \cos(n\omega t + \Delta\varphi_n) & -\sin(n\omega t + \Delta\varphi_n) \\ \sin(n\omega t + \Delta\varphi_n) & \cos(n\omega t + \Delta\varphi_n) \end{bmatrix} \quad (10)$$

## III. SIMULATION RESULTS

### A. SIMULATION OF HARMONIC CURRENT DETECTION METHOD

The simulation model of the harmonic currents detection method proposed in this paper is built on the PSIM platform.

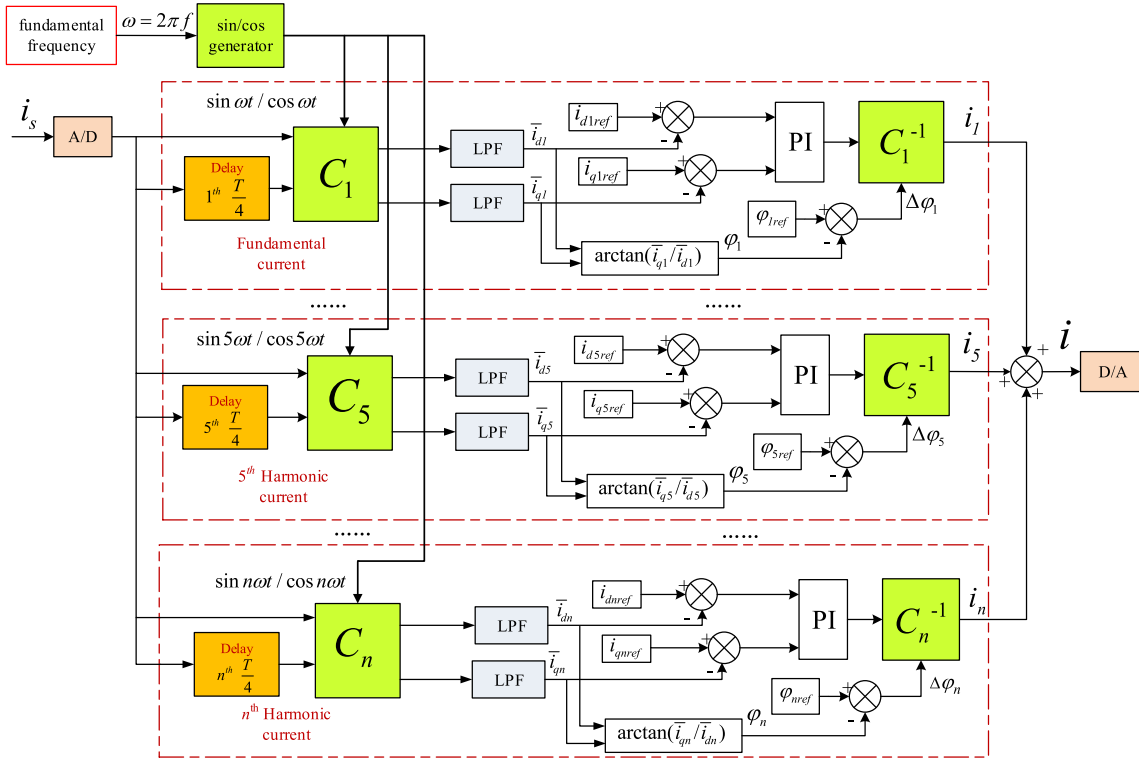


FIGURE 9. Operation flow of MHCIS.

TABLE 2. Simulation parameters of harmonic currents.

Harmonic order	Amplitude(A)	Phase angle(°)
1	5	20
5	10	60

The parameters design of LPF will influence the dynamic response and precision of the system, so a second-order LPF is used in this system and the cut-off frequency is 25 Hz, considering the trade-off between the accuracy and dynamic response. Table 2 shows the simulation parameters.

The simulation results of the detected amplitudes and phase angles for the fundamental and 5<sup>th</sup> harmonic current are shown in Figs.10 and 11, from which it can be seen that the selective harmonic current amplitude and phase angle can be detected accurately within 20-40ms. The ripples shown in the phase angle detection results are caused by the characteristics of the LPF.

The simulation results show that the selective harmonic current detection algorithm proposed in this paper can meet the MHCIS’s requirements for dynamic response.

**B. SIMULATION OF HARMONIC CURRENT DETECTION STRATEGY**

In order to verify the effectiveness of the proposed selective harmonic current detection and control method, the simulation model of MHCIS has been built on the PSIM platform,

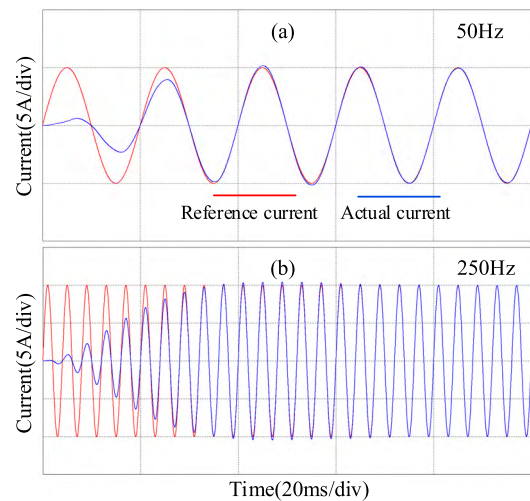


FIGURE 10. Harmonic current amplitude detection results: (a) Fundamental current (b) 5<sup>th</sup> harmonic current.

and a single phase inverter model with dual closed-loop control has been designed. Table 3 gives the detailed simulation parameters of the MHCIS.

The fundamental and 7<sup>th</sup> harmonic currents are taken for examples, and the parameters of harmonic currents are given in Table 4. Fig.12 shows the simulation results of single order harmonic current, from which we can find that the harmonic current can be detected and controlled accurately within 1-2 fundamental cycles.

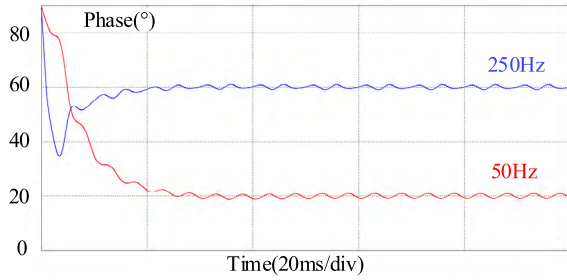


FIGURE 11. Detection results of phase angle for respective harmonic current.

TABLE 3. Simulation parameters of the MHCIS.

Parameters	Value
Fundamental Frequency	50Hz
Switching Frequency	25000Hz
$V_{DC}$ (Amplifier)	180V
Filter Capacitor	33 $\mu$ F
Filter Reactor	64 $\mu$ H
Tested Capacitor	0.6mF

TABLE 4. Parameters of harmonic current.

Harmonic order	Amplitude(A)	Phase angle(°)
1	10	0
7	5	0

TABLE 5. Parameters of the superposed harmonic currents.

Harmonic order	Amplitude(A)	Phase angle(°)
1	10	70
3	3.3	42

However, it is far from enough to show the effectiveness of the proposed control strategy for MHCIS. Thus the fundamental current and the 3<sup>rd</sup> harmonic current are superposed and then injected into the power capacitors to verify the feasibility of the current control algorithm. The detailed parameters of the multiple harmonic currents are shown in Table 5.

The simulation results of multiple harmonic currents are shown in Figs. 13 and 14. In order to make a comparison, Fig. 13 shows the results that the phase angle is compensated, while the results that the phase angle is uncompensated are shown in Fig. 14.

#### IV. EXPERIMENTAL RESULTS

In the process of the experiment, harmonic power supply generates multiple harmonic currents and its output frequency ranges from 0 to 2.5 kHz. As shown in Fig. 2, the RT-LAB hardware-in-the-loop simulation platform OP5600 is used in the experiment. The dynamic system mathematical model of Matlab/Simulink can be directly compiled and imported into RT-LAB for real-time control and testing. It can be regarded as the signal generator, ADC (Analog-Digital Converter),

TABLE 6. Interface parameters of RT-LAB.

Analog Input Module	Analog Output Module
16-bit ADC	16-bit DAC
Up to 16 Channels	Up to 16 Channels
Updating rate up to 500K/s	Updating rate up to 1M/s

TABLE 7. Parameters of the comparative experiments.

Harmonic order	Amplitude(A)	Compensation phase angle(°)
1	10	-70
3	5	-42

TABLE 8. Reference values of the harmonic currents.

Harmonic order	Amplitude(A)	Compensation phase angle(°)
1	5	-70
5	1.22	-11
7	4	8
13	13	53.5

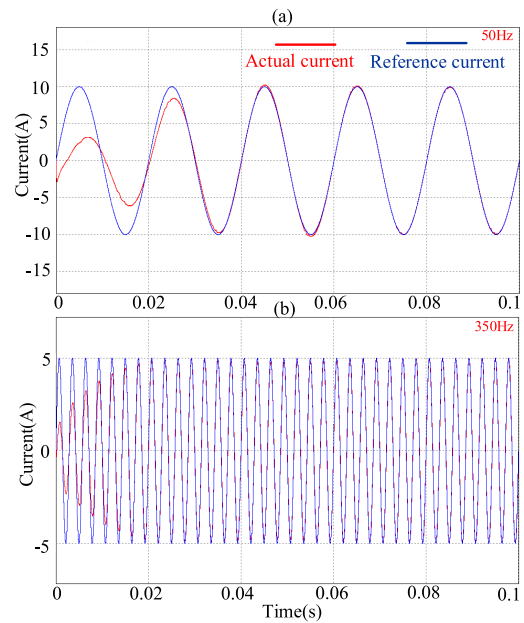


FIGURE 12. Simulation results of current control: (a) Fundamental current control (b) 7<sup>th</sup> harmonic current control.

DAC (Digital-Analog Converter) and controller. Some important interface parameters of RT-LAB are shown in Table 6.

The fixed step size of the system is 1/20k and the sampling rate is 20 kHz. The frequency, amplitude and phase angle of the reference current can be set up in the host computer, and the experimental platform is shown in Fig. 15.

To verify the validity of the phase angle compensation strategy, the comparative experiments are carried out. The detailed parameters about the experiments are shown in Table 7.

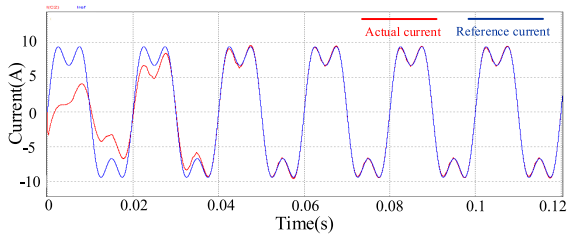


FIGURE 13. Simulation results of compensated phase.

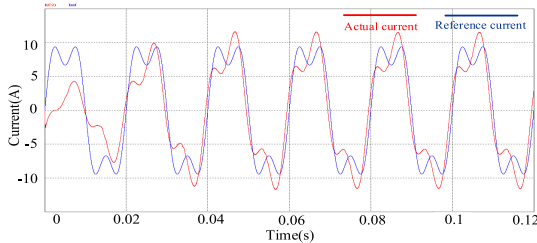


FIGURE 14. Simulation results of uncompensated phase.

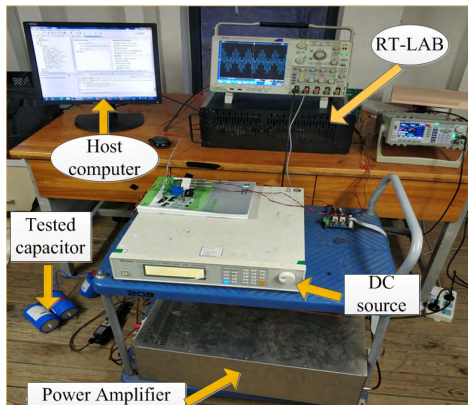


FIGURE 15. Experimental platform.

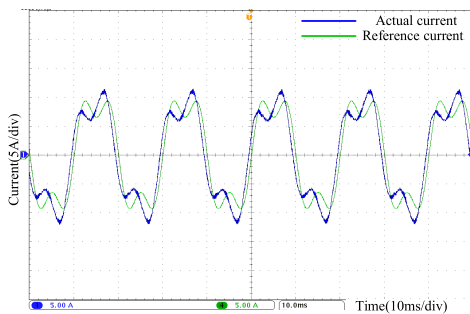


FIGURE 16. Experimental results of the uncompensated phase.

Figs. 16 and 17 show the results that the phase angles are uncompensated and compensated respectively. Fig.16 shows the distortion of the output current due to the system impedance associated to the frequency. As shown in Fig.17, the output current is symmetric because of the compen-

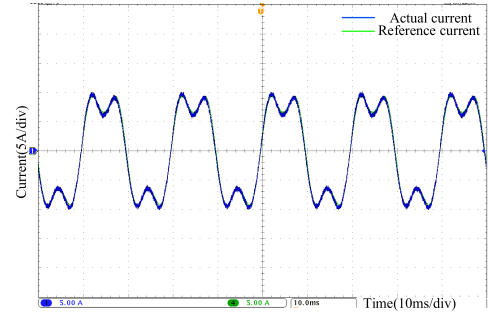


FIGURE 17. Experimental results of the compensated phase.

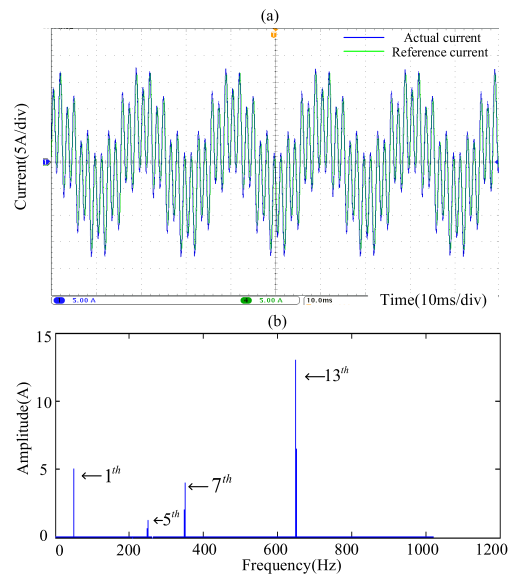


FIGURE 18. Experiment results of the harmonic currents injection system: (a) harmonic currents injected into the power capacitor (b) the spectrum of the injected currents.

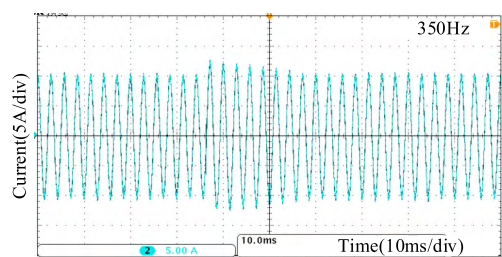


FIGURE 19. Results of the abrupt load changing experiment.

sated phase angle. The compensated phase angle is shown in Table 7.

Due to the limitation of experimental bench in the laboratory, the reference values of several typical harmonic currents are shown in Table 8. In the pretreatment segment, the phase offset of the corresponding harmonic current is detected, calculated and used for the compensation.

After the compensation of phase angle for each harmonic current, the MHCIS designed in this paper can steadily and accurately output the multiple harmonic currents.

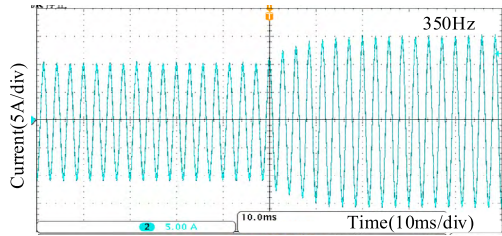


FIGURE 20. Results of the reference amplitude modification experiment.

The multiple harmonic currents that are injected into the tested capacitors are shown in Fig. 18 (a), and Fig. 18 (b) shows the results of spectrum analysis. As shown in the spectrum, the amplitudes of the fundamental current, 5<sup>th</sup> harmonic current, 7<sup>th</sup> harmonic current and 13<sup>th</sup> harmonic current are about 4.98A, 1.2A, 4A, and 13.1A, respectively. It is obvious that the output currents have the same harmonic components compared to the reference currents.

To prevent the harmful effects of sudden changes of experimental environment parameters on the system, it is necessary to verify the robustness and dynamic response of the MHCIS. Then the abrupt load changing experiment and the reference amplitude modification experiment are carried out. Fig. 19 shows the results of the abrupt load changing experiment, where the load is changed from 400 $\mu$ F to 600 $\mu$ F. It can be found that the current will be stabilized after a sudden increase and the dynamic response is about 30ms. Then Fig.20 shows the results of the reference amplitude modification experiment, where the reference amplitude of the current is changed from 10A to 15A, and the output current can follow the reference value within 20-30ms. The experimental results show that dynamic response of the proposed current control strategy can meet the requirements of the audible noise analysis for AC filter capacitor.

## V. CONCLUSION

This paper proposes a selective harmonic current detection and control algorithm for MHCIS to analyze the noise characteristics of AC filter capacitors. Based on the instantaneous reactive power theory, the transformation relation between the stationary frame and synchronous rotating frame is derived. In the preprocessing stage, it is essential to compensate the phase offset caused by the system inherent delay.

The mathematical analysis and simulation results confirm that the proposed selective harmonic current detection strategy can accurately and timely detect the magnitude and phase angle of each harmonic current.

The simulation results of MHCIS also show that the paralleled PI regulators in multiple synchronous rotating coordinate systems are sufficient to provide zero steady-state error. Finally, the experimental results validate that the MHCIS designed in this paper can be applied to the audible noise analysis for AC filter capacitors.

## REFERENCES

- [1] M. Barnes, D. Van Hertem, S. P. Teeuwsen, and M. Callavik, "HVDC systems in smart grids," *Proc. IEEE*, vol. 105, no. 11, pp. 2082–2098, Nov. 2017.
- [2] *High Voltage Direct Current (HVDC) Substation Audible Noise*, document IEC 22F/83/NP: 30-33, 2009.
- [3] J. Li, L. Zhu, S. Ji, H. Cui, and Y. Shi, "Vibration analysis of power capacitors and vibration reduction with damping structures," in *Proc. IEEE Int. Power Modulator High Voltage Conf. (IPMHVC)*, San Francisco, CA, USA, Jul. 2016, pp. 107–112.
- [4] M. D. Cox and H. H. Guan, "Vibration and audible noise of capacitors subjected to nonsinusoidal waveforms," *IEEE Trans. Power Del.*, vol. 9, no. 2, pp. 856–862, Apr. 1994.
- [5] L. Zhu, J. Li, Y. Shi, H. Rehman, and S. Ji, "Audible noise characteristics of filter capacitors used in HVDC converter stations," *IEEE Trans. Power Del.*, vol. 32, no. 5, pp. 2263–2271, Oct. 2017.
- [6] S. Jain, P. Agarwal, H. O. Gupta, and G. Agnihotri, "Modeling of frequency domain control of shunt active power filter using MATLAB simulink and power system blockset," in *Proc. Int. Conf. Electr. Mach. Syst.*, Nanjing, China, 2005, pp. 1124–1129.
- [7] S. M. Williams and R. G. Hofit, "Adaptive frequency domain control of PWM switched power line conditioner," *IEEE Trans. Power Electron.*, vol. 6, no. 4, pp. 665–670, Oct. 1991.
- [8] S. Zheng, G. Yao, J. Han, T. Tang, and X. Han, "Frequency-domain current control of harmonic current injection system for power capacitor," in *Proc. IEEE Int. Power Electron. Appl. Conf. Exposit. (PEAC)*, Shenzhen, China, Nov. 2018, pp. 1–6.
- [9] H. Akagi, Y. Kanazawa, and A. Nabae, "Instantaneous reactive power compensators comprising switching devices without energy storage components," *IEEE Trans. Ind. Appl.*, vols. IA–20, no. 3, pp. 625–630, May 1984.
- [10] W. Jiang, D. Zhao, Y. Zhang, Y. Hu, and L. Wang, "Different control objectives for grid-connected converter under unbalanced grid voltage using forgotten iterative filter as phase lock loop," *IET Power Electron.*, vol. 8, no. 9, pp. 1798–1807, Sep. 2015.
- [11] F. Zheng Peng, G. W. Ott, and D. J. Adams, "Harmonic and reactive power compensation based on the generalized instantaneous reactive power theory for three-phase four-wire systems," *IEEE Trans. Power Electron.*, vol. 13, no. 6, pp. 1174–1181, Nov. 1998.
- [12] T.-S. Lee and J.-H. Liu, "Modeling and control of a three-phase four-switch PWM voltage-source rectifier in d-q synchronous frame," *IEEE Trans. Power Electron.*, vol. 26, no. 9, pp. 2476–2489, Sep. 2011.
- [13] W. Jing, L. Di-chen, L. Pan, and Z. Jie, "A new algorithm for random harmonic current detection based on mathematical morphology," in *Proc. WRI Global Congr. Intell. Syst.*, Xiamen, China, 2009, pp. 365–369.
- [14] J. Liu, J. Yang, and Z. Wang, "A new approach for single-phase harmonic current detecting and its application in a hybrid active power filter," in *Proc. 25th Annu. Conf. IEEE Ind. Electron. Soc.*, San Jose, CA, USA, Oct. 1999, pp. 849–854.
- [15] A. G. Yepes, F. D. Freijedo, J. Doval-Gandoy, Ó. López, J. Malvar, and P. Fernandez-Comesaña, "Effects of discretization methods on the performance of resonant controllers," *IEEE Trans. Power Electron.*, vol. 25, no. 7, pp. 1692–1712, Jul. 2010.
- [16] C. Zou, B. Liu, S. Duan, and R. Li, "Stationary frame equivalent model of proportional-integral controller in dq synchronous frame," *IEEE Trans. Power Electron.*, vol. 29, no. 9, pp. 4461–4465, Sep. 2014.
- [17] B. Bahrani, S. Kenzelmann, and A. Rufer, "Multivariable-PI-Based dq current control of voltage source converters with superior axis decoupling capability," *IEEE Trans. Ind. Electron.*, vol. 58, no. 7, pp. 3016–3026, Jul. 2011.
- [18] S. Xu and J. Xu, "A current decoupling parallel control strategy of single phase inverter with voltage and current dual closed-loop feedback," *IEEE Trans. Ind. Electron.*, vol. 60, no. 4, pp. 1306–1313, Apr. 2013.
- [19] P. Mattavelli and F. P. Marafao, "Repetitive-based control for selective harmonic compensation in active power filters," *IEEE Trans. Ind. Electron.*, vol. 51, no. 5, pp. 1018–1024, Oct. 2004.
- [20] A. Nami, J. Amenedo, S. Gómez, and M. Álvarez, "Active power filtering embedded in the frequency control of an offshore wind farm connected to a diode-rectifier-based HVDC link," *Energies*, vol. 11, no. 10, p. 2718, 2018.
- [21] Y. Zhang, Y. W. Li, N. R. Zargari, and Z. Cheng, "Improved selective harmonics elimination scheme with online harmonic compensation for high-power PWM converters," *IEEE Trans. Power Electron.*, vol. 30, no. 7, pp. 3508–3517, Jul. 2015.

- [22] *Acoustics—Determination of Sound Power Level and Directivity Character of Power Capacitor Unit Using Sound Pressure—Part 1: Precision Method for Hemi-Anechoic Rooms*, document GB/T 32524.1-2016, 2016.
- [23] X. Han, J. Han, G. Yao, and T. Tang, "Current control strategy of harmonic current injection system for power capacitor," in *Proc. IEEE 27th Int. Symp. Ind. Electron. (ISIE)*, Cairns, QLD, Australia, Jun. 2018, pp. 366–371.
- [24] S. Golestan, J. M. Guerrero, and J. C. Vasquez, "Single-phase PLLs: A review of recent advances," *IEEE Trans. Power Electron.*, vol. 32, no. 12, pp. 9013–9030, Dec. 2017.
- [25] P. Yang, L. Deng, *Parameter Tuning Method and Application of PID Controller*. Beijing, China: Electric Power Press, 2016, pp. 9–19.
- [26] W. Khuen Ho, C. Chieh Hang, and J. Zhou, "Self-tuning PID control of a plant with under-damped response with specifications on gain and phase margins," *IEEE Trans. Control Syst. Technol.*, vol. 5, no. 4, pp. 446–452, Jul. 1997.
- [27] A. S. Deshmukh and S. R. Vaishnav, "A comparative performance analysis of PID tuning techniques based on frequency response specification," in *Proc. 2nd Int. Conf. Emerg. Trends Eng. Technol.*, 2009, pp. 971–974.



converter, multilevel converter, and renewable energy.

**JINGANG HAN** (Member, IEEE) received the B.Eng. and Ph.D. degrees in electrical engineering from Shanghai Maritime University, Shanghai, China, in 2001 and 2007, respectively. Since 2007, he has been an Associate Professor with the Department of Electrical Automation, Shanghai Maritime University. From 2011 to 2012, he was a Postdoctoral Research Fellow with the French Naval Academy, Brest, France. His research interests include analysis, design, and control of power



**SHOUZHI ZHENG** is currently pursuing the master's degree in electrical engineering with Shanghai Maritime University, Shanghai, China. His current research interests include renewable energy and harmonic detection.



an Assistant Professor. He is responsible for and attends several research projects. He has authored/coauthored more than 40 journal articles and conference papers. His research interests include sustainable energy generation systems and power conversion, onboard power systems, intelligent control and power management of microgrid, fault diagnosis, and fault tolerant control.

**GANG YAO** (Member, IEEE) received the M.Eng. and Ph.D. degrees in electrical engineering from Shanghai Maritime University, Shanghai, China, in 2004 and 2008, respectively. From January 2008 to August 2009, he was a Postdoctoral Research Fellow with the University of Nantes, France. Since December 2009, he has been with the Department of Sino-Dutch Mechatronics Engineering, Shanghai Maritime University, where he is currently the Chair with the Department and



trical machines, and wind or tidal energy conversion systems.

**HAO CHEN** (Member, IEEE) received the B.E. degree in automation from Shanghai Maritime University, Shanghai, China, in 2008, and the M.S. and Ph.D. degrees in electrical engineering from the University of Nantes, Nantes, France, in 2010 and 2014, respectively.

From 2014 to 2016, he held a postdoctoral position with Shanghai Maritime University, where he is currently a Lecturer. His research interests include designing, modeling, and control of electrical machines, and wind or tidal energy conversion systems.



currently a full-time Professor with the Ecole Polytechnique de l'Université de Nantes (Polytech Nantes). He is also the Director of research with Polytech Nantes. He is also in charge of the collaborations between Polytech Nantes and Chinese universities. He has also coordinated or managed 15 National or European collaborative research programs. He has authored or coauthored seven chapters in four scientific books, 50 journal articles, and more than 100 national or international conferences. His research interests include array signal processing, spectral analysis, and mobile wireless communication systems.

**YIDE WANG** (Senior Member, IEEE) received the B.S. degree in electrical engineering from the Beijing University of Post and Telecommunication, Beijing, China, in 1984, and the M.S. and Ph.D. degrees in signal processing and telecommunications from the University of Rennes, France, in 1986 and 1989, respectively. From 2008 to 2011, he was the Director of the Regional Doctorate School of Information Science, Electronic Engineering and Mathematics. He is currently



applications.

**TIANHAO TANG** (Senior Member, IEEE) was born in Jiangsu, China, in 1955. He received the B.Sc. and M.Sc. degrees in electrical engineering from the Shanghai University of Technology, Shanghai, China, in 1982 and 1987, respectively, and the Ph.D. degree in control engineering from Shanghai University, Shanghai, in 1998.

From 1988 to 1991, he was a Lecturer with Shanghai Maritime University, Shanghai, where he was an Associate Professor and a Professor, in 1992 and 1998, respectively. He is currently the Director of the Institute of Electric Drives and Control Systems, Shanghai Maritime University, and the Vice Director of the Sino-French Joint Research Institute of Galileo and Maritime ITS for Safer Seas. His main research interests are in intelligent control, electrical propulsion systems, and power electronics in renewable

...